

Inhibition performance of 2-(Dibutylamino)-4,6-Dimercapto-1,3,5-Triazine self-assembled film for copper corrosion in 3.5 wt% NaCl solutions

Hailiang Guo¹, Shengtao Zhang^{1,*}, Xu Wang¹, Chaohui Liao¹, Yanan Wen¹, Jiayu Luo²,
Lingfeng Wang², Shijin Chen³

¹School of Chemistry and Chemical Engineering, Chongqing University, Chongqing 400044, China.

²School of Materials and Energy and Center for Applied Chemistry, University of Electronic Science and Technology of China, Chengdu 610054, P. R. China

³Research and Development Department, Guangdong BominSci-Tech Co., Ltd., Meizhou 514000, P. R. China.

*E-mail: stzhang_cqu@163.com

Received: 9 April 2019/ Accepted: 15 May 2019 / Published: 30 June 2019

The printed circuit board (PCB) acts as a carrier for various components to achieve interconnection and interconnection with each other. Therefore, the protection of copper on the surface of PCB is very important. It is of great practical significance to quest the approach to reduce the corrosion of copper in the chloride ion environment. The film of 2-(Dibutylamino)-4,6-Dimercapto-1,3,5-Triazine (MSDS) fabricated by self-assembly on a copper surface can prevent copper corrosion in a 3.5% NaCl solution. Electrochemical testing, morphological characterization and theoretical calculations were used to study its inhibition mechanism and performance. The results display that MSDS modified copper has better corrosion inhibition performance than 2,4,6-trimercapto-1,3,5-triazine (TMTA) modified copper in 3.5% NaCl solution, and the corrosion resistance of MSDS SAMs reaches 97.91%, this shows that MSDS has more excellent corrosion resistance in triazines.

Keywords: PCB; Copper; Corrosion; Self-assembled film

1. INTRODUCTION

Printed circuit boards (PCB) require high conductive lines to form at room temperature on substrates such as polytetrafluoroethylene (PTFE), especially in the Fifth generation mobile communication network (5G) era, the requirements for signal integrity are getting higher and higher, which is crucial for the protection of wire. In the past, due to the price advantage of copper nanoparticles and the excellent conductivity, it has always been the first choice for high-conductivity

circuits in the PCB.[1-2] However, the corrosion problem of copper cannot be ignored, especially in the presence of chloride ions, which is highly susceptible to corrosion. Copper corrosion inhibition has become a hot topic in society and is worth studying, especially in Marine environment.[3-7] Self-assembled monolayer is thin film that can adsorb metal surfaces spontaneously. It is usually only 1-3 nanometers. Many reports have shown that self-assembled films have the function of inhibit corrosion of the metal surface.[8-11]

Numerous organic compounds have been deemed to be adsorptive inhibitors for metal corrosion, such as fatty acid, thiol, dithiol, and some other heterocyclic compounds which contain N, S, atoms. [12-18] In addition, alkyl chain is also beneficial to enhance the inhibition of organic compounds.[19-20] Therefore, in this work, adsorb MSDS on the copper surface. The result of SAMs was also characterized by the Fourier Transform Infrared (FT-IR), contact angle (CA), scanning electronic microscope (SEM), and atomic force microscope (AFM). Then, the effect of immersion time on film formation was studied by electrochemical experiments. Finally, the relationship between molecular structure and adsorption mechanism was analyzed by means of quantum chemical calculation.

2. EXPERIMENTAL SECTION

2.1. Materials and chemicals

MSDS (purity > 95.0%, Chemical Industry Co., Ltd, Tokyo, Japan). The molecular structure of MSDS is shown in Fig 1. TMTA (purity > 95.0%, Titan Scientific Co., Ltd, Shanghai, China). All of the drugs involved were at the analytical level. Sodium chloride (NaCl, 99.5wt%, Xilong science Ltd), absolute ethanol (C_2H_5OH , 99.7%, Guanghua Sci-Tech Co., Ltd, Guangdong, China), acetone (CH_3COCH_3 , 99.5%, Xilong science Ltd), encapsulate the copper block with epoxy resin and the bare leakage area is 1cm^2 that act as working electrodes. Before the SAM preparation and other tests were carried out, the copper surface was polished step by step with different grades of sandpaper that make copper surface flat, polish the copper surface as smooth as a mirror with polishing powder. Next, rinse and skim them respectively with ultrapure water and acetone and anhydrous ethanol for 5 minutes. Finally, samples are dried by a plasma cleaner in a nitrogen atmosphere (p15v Boffotto. Ltd. Zhuhai).

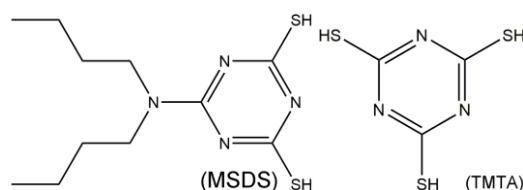


Figure 1. Molecular structure of MSDS and TMTA.

2.2. Preparation of MSDS SAMs

At different times, soak freshly prepared copper samples in different concentrations of solution. After that, removed and washed them with a large amount of water. Then immerse these

samples in anhydrous ethanol. The course must be lasting one minute in order to remove the drug adsorbed physically on the copper surface. Other contrast tests involving self-assembled membranes have maintained the same operation.

2.3. The surface structure

Whether the MSDS assembles successfully on the surface of copper is measured by the Fourier Transform Infrared (FT-IR Thermo Scientific Nicolet iS10 Pittcon America). The ATR is used to measure the copper samples and the wave number ranges from 650 to 4000 cm^{-1} . The IR collects the number of the MSDS powder of 400-4000 cm^{-1} , otherwise, the spectral resolution was 2 cm^{-1} .

2.4. Electrochemical measurement

Copper electrodes were applied as working electrodes with and without self-assembled film, 4 square centimeters of platinum were used as counter electrode, the reference electrode is a common saturated calomel electrode (SCE) that is attached to the Lugin capillary, which minimizes chloride interference. The all electrochemical measurements were performed by means of the CHI660E workstation using the three-electrode system at 298 K.

2.5. Surface morphology analysis

Scanning electron microscopy (SEM, TM-4000PLUS, HITACHI, Japan) and atomic force microscopy (AFM, MFP-3D-BIO, Asylum Research, America) were used to study the copper morphology in different cases. Contact angle of water on bare copper and MSDS modified copper by contact angle goniometer (CA, SL150, Solon Information Technology Co., Ltd, Shanghai) by a standing drop method, and the size of the water droplets was 5 μl . In order to avoid the occurrence of contingency in the measured CA value, at least four measurements of different points of the same sample were investigated.

2.6. Quantum chemical calculations and molecular dynamics (MD) simulations

Quantum chemical calculations were performed based on Gaussian 03 W software. Density functional theory (DFT) was used to optimize the molecular structure of MSDS based on B3LYP functional theory and 6-311+ G (d, p). The relevant parameters of quantum chemistry are the energy containing the highest occupied molecular orbital (E_{HOMO}) and the lowest unoccupied molecular orbital (E_{LUMO}), μ (dipole moment).

The adsorption mechanism of MSDS on Cu surface was executed via Molecular dynamics (MD) simulations using Accelrys Inc's Forcite module. The reason why choose surface Cu(111) as representative is that it has strong stability and low Miller index. Suppose that in a three-dimensional box, the size of the (2.2 nm \times 2.6 nm \times 4.3 nm) simulated inhibitor interacts with the copper surface,

accompanied by a 298k compass field with a cyclic front. MD simulation is performed under the simulation temperature 298K and NVT specifications, time step 1fs, simulation time 1000ps.

3. RESULTS AND DISCUSSION

3.1. Fourier transform infrared spectroscopy (FT-IR)

Fourier transform infrared spectroscopy (FT-IR) is commonly used to determine some structures of SAMs.[21-23] The FT-IR spectrum of the high purity MSDS and the copper surface after 12 hours of soaking in 2 mM MSDS solution is shown in Figure 2. The spectrum of MSDS shows the appearance of ν N-H stretching bands at 3339-2845 cm^{-1} , in addition, there is also the expansion and contraction of C-H. The bands at 1431 and 1457 cm^{-1} correspond to ν R, and the bands at 1126 cm^{-1} associate to ν R coupled with the ν N-H and δ C=S. The band at 1596, which is typical bands for MSDS in aromatic form, can be described as an N-H in-plane peak. Further, there are two weak bands at 1273 and 1193 cm^{-1} , which are an inactive areas of infrared light. Obviously, they can be ascribed to the symmetric mode of ν C=S and the ν R. The MSDS SAMs on the copper surface still has a similar profile compared to the pure MSDS (b) spectrum. These corresponding peaks indicate that the MSDS molecules have been adsorbed and assembled on the copper surface. There are some slight deviations in the summit due to the adsorption behavior that forms the Cu-MSDS complex, resulting in some band offsets and fractures.

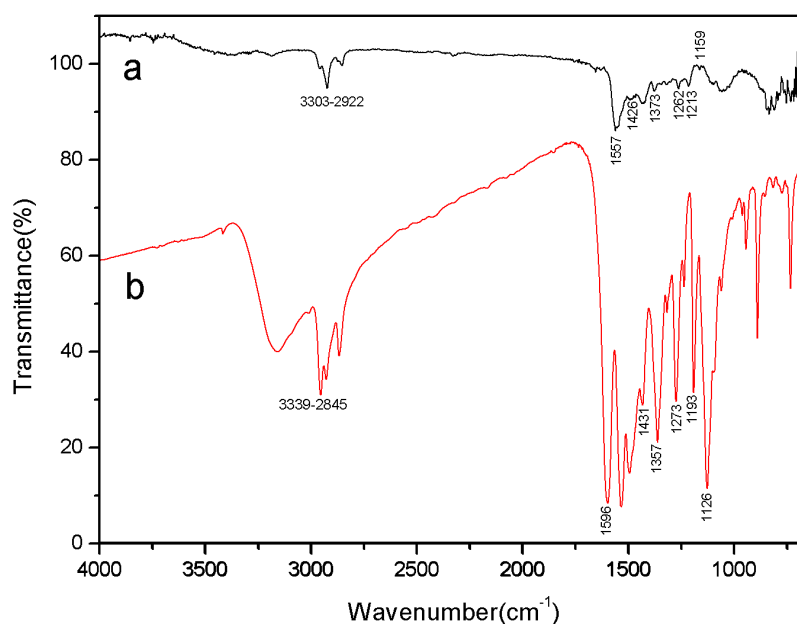
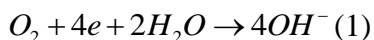


Figure 2. Fourier transform infrared (FT-IR) spectra : (a)MSDS modified copper surface and (b) the MSDS powder

3.2. Potentiodynamic polarization curves

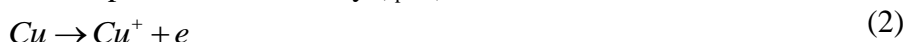
Fig.3c,3d show the dynamic polarization curves of copper measured in 3.5wt% NaCl solution, and the copper was not immersed in the same MSDS solutions meanwhile. Anode and cathode reactions of copper in sodium chloride solution have been reported in many literatures.[24-27]

The cathodic reaction can be described simply by



Relatively, the anodic reaction is a complex multi-step reaction.

(a) Cu(0) is oxidized to Cu(I) (Eq. (2)), In Fig.3a,3b, This step is the transition from low anode potential to the peak current density (i_{peak})



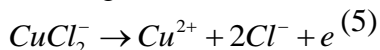
(b) Then in the presence of Cl^- , Cu(I) rapidly forms an insoluble film CuCl (Eq. (3)). The current density decreases from maximum (i_{peak}) to a minimum (i_{min}) (Fig. 3a,3b)



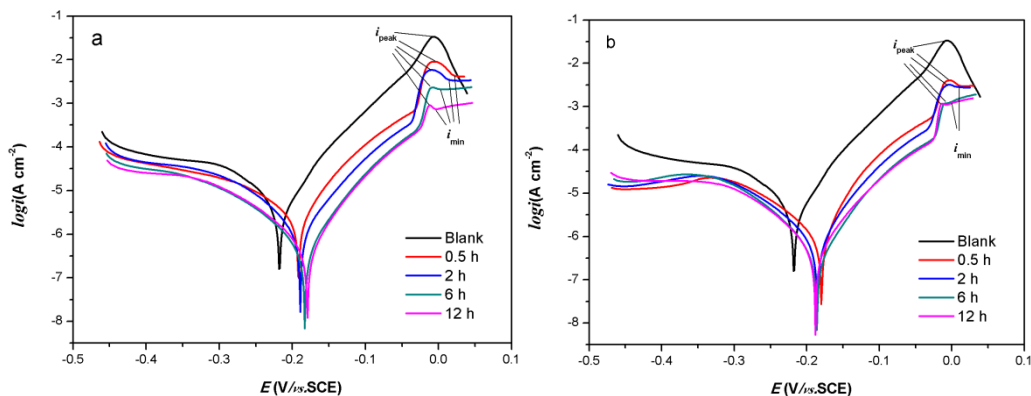
(c) The adsorption film composed of copper chloride cannot effectively prevent attack of corrosive media because of formation of soluble cuprous chloride complex ($CuCl_2^-$) (Eq. (4)) increased with concentration of Cl^- . Following that, the current density begins to rise again from i_{min} (described in Fig.3a,3b)



(d) $CuCl_2^-$ Ions break off the surface and enter the solution, then Cu^+ oxidize into Cu^{2+} (Fig. 3a,3b) and the current density increases again.



The current decreased significantly with the increase of self-assembly time and solution concentration in Fig.3a,3b. This indicates that MSDS SAMs can effectively inhibit the oxidation of copper, and inhibit the diffusion of dissolved oxygen and chloride ions to the surface of copper, the anode melting of copper is gradually inhibited. At the same time, the cathode current also decreased to a small extent, indicating that MSDS SAMs can also inhibit the dissolution of copper by weakening the occurrence of cathode reaction, which confirmed that MSDS SAMs is a mixed molecular membrane. These can be observed from changes in the polarization curve in Fig.3a,3b.



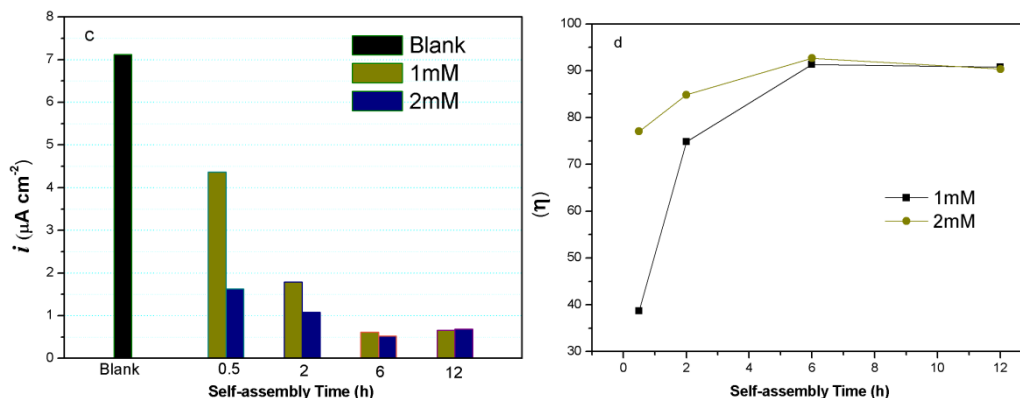


Figure 3. (a) Potentiodynamic polarization curves of MSDS (1 mM) and (b) MSDS (2 mM) modified copper electrode immersed in 3.5 wt% NaCl solution corresponding different self-assembly times at 298 K, (c) corrosion current density and (d) Inhibition effect of modified copper samples under different conditions.

In order to more clearly see the influence of MSDS self-assembly time and concentration on copper corrosion, the core data corrosion current (i_{corr}) and corrosion efficiency (η) are made into in Fig.3c,3d. respectively. The corrosion current decreases with the extension of self-assembly time, and the concentration has a significant influence on the corrosion current in the case of short self-assembly time. The copper electrode was assembled in 1mM MSDS solution with 0.5h corrosion current of $4.369 \mu\text{A cm}^{-2}$, at same self-assembly time, the corrosion current is greatly reduced to $1.636 \mu\text{A}$. As the prolonging of self-assembly time goes by, the influence of concentration becomes smaller and smaller. When the self-assembly time reaches six hours, the corrosion current changes little and the corrosion efficiency reaches the maximum, 90.79% and 90.36%, at both concentrations (1mM and 2mM), the corrosion inhibition efficiency (η^0) obtained by the driven potential polarization curve was calculated by the Eq (6).

$$\eta(\%) = \frac{I_{corr}^0 - I_{corr}}{I_{corr}^0} \times 100\% \quad (6)$$

where I_{corr}^0 and I_{corr} indicate the current density of unmodified copper and modified copper samples, respectively.

3.3. EIS measurement

The application of electrochemical impedance spectroscopy has been widely reported in the study of electrochemical corrosion. The Nyquists of bare copper and modified copper samples obtained in 3.5 wt% NaCl solution under different conditions are depicted in Figs.4. The bare copper Nyquist impedance diagram displays a sunken semicircle at high frequency (HF), then, there is a significant linear representing the Warburg impedance, located in low frequency (LF) region. The charge transfer during copper dissolution is reflected on the semicircle. [28-30] Generally, there are two main explanations for the formation of LF linear regions, there are two possibilities: first, Diffusion of aerobic molecules on copper surface, another, migration of other corrosive ions such as soluble

corrosion products $CuCl_2^-$ at the copper/solution interface. Compared with bare copper, the capacitance loop diameter of MSDS modified copper is significantly increased, indicating that MSDSSAMS has good inhibition of copper corrosion in neutral chloride. On the other hand, also found that with the addition of MSDS, warburg impedance completely disappeared, which indicated that under the condition that MSDSSAMS was sufficiently dense, the diffusion process was strongly inhibited. In the same case, other triazine substances were selected for electrochemical impedance comparison, the capacitance was smaller than the previous one, and the Warburg impedance still existed. The impedance diagram is shown in the Fig.5. Many studies have shown that substances containing N generally inhibit the corrosion of copper in chloride solutions.

Figs.6 is an equivalent circuit of the system, Fig.6a, fitting the impedance spectrum in the case of Warburg impedance, and Fig.8a is used for other spectra. Herein, R_{ct} represents a charge transfer resistance, and W signifies Warburg impedance. R_s and R_f stand for the resistance of the solution and the resistance of the self-assembled absorbed film on the copper surface, respectively. CPE_f and C_{dl} token film capacitors and double layer capacitors, respectively.[29-32]

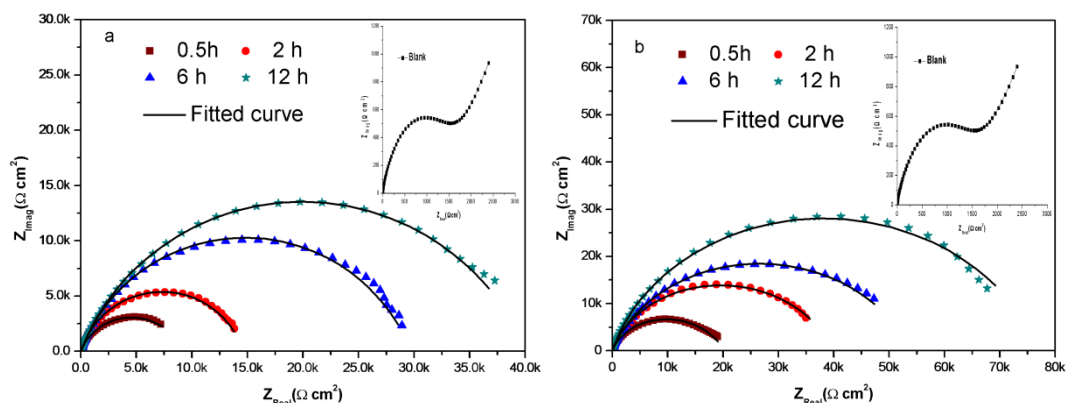


Figure 4. Nyquist plots: MSDS(a) (1 mM) and MSDS(b) (2 mM) were immersed in 3.5 wt% NaCl solution at 298 K to modify the copper electrodes With different modification times.

The impedance relevant parameters (pictured in Table 1 and 2) are calculated via equivalent circuit. The suppression efficiency (η) is calculated from the charge transfer resistance (R_{ct}) obtained from EIS, and the relationship is as follows

$$\eta(\%) = \frac{R_{ct} - R_{ct}^0}{R_{ct}} \times 100\% \quad (7)$$

where R_{ct} and R_{ct}^0 are the charge-transfer resistances of bare copper and modified copper specimens, respectively.

Compared with bare copper, the R_{ct} value after MSDS transformation is significantly increased. This indicates that the formed MSDS SAMs has excellent performance in copper corrosion protection. Furthermore, with the introduction of SAM, the values of C_f and C_{dl} are reduced, which can be attributed to the use of smaller exposed electrode surface areas by replacing the water molecules by the inhibitor molecules studied.[30] As the assembly time increases, more MSDS molecules adsorb on the

copper surface, resulting in an increase in the coverage area of the protective film, generating an increase in the thickness of the dielectric double layer and a decrease in the local dielectric constant. In addition, as the concentration of MSDS and the self-assembly time increases, Corrosion inhibition efficiency is significantly improved. When the MSDS concentration was 2 mM and the self-assembly time was 6 hours and 12 hours, the inhibition efficiency reached 97.02% and 97.91%, respectively, which were very close. This indicates that the system reached adsorption equilibrium after 12 hours, and the self-assembly time coincided with the results of the polarization curve measurement.

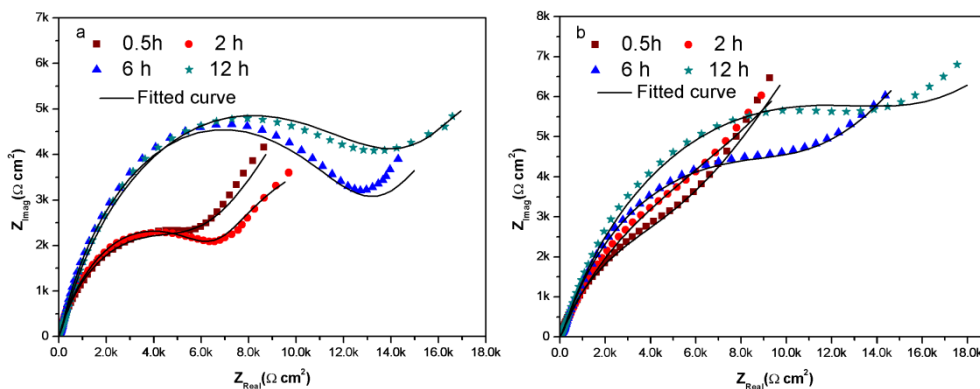


Figure 5. Nyquist plots: TMTA (1 mM) (a) and TMTA (b) (2 mM) were immersed in 3.5 wt% NaCl solution at 298 K to modify the copper electrodes With different modification times.

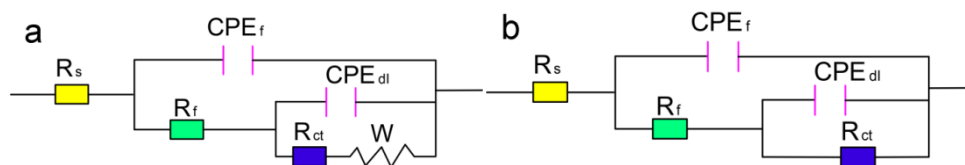


Figure 6. Fitting the experimental data of copper electrode in seawater environment with equivalent circuit diagram.

Table 1. Impedance parameters of bare copper and MSDS modified copper in 3.5wt% NaCl solution

C (mM)	Time(h)	$R_s(\Omega \text{ cm}^2)$	$Q_{film}(S\text{sn}\text{cm}^{-2})$	n_1	$R_{film}(\Omega \text{ cm}^2)$	$Q_{dl}(S\text{sn}\text{cm}^{-2})$	n_2	$R_{ct}(\Omega \text{ cm}^2)$	W	$\eta(\%)$	
Bare		0.602	1.095×10^{-5}	1	105.8	1.21×10^{-4}	0.618	1.61×10^3	0.005968	/	
MSDS-SAMS	1	0.5	8.892×10^{-5}	0.688	23.26	8.89×10^{-4}	0.907	9.23×10^3	/	82.56	
		2	0.655	1.831×10^{-5}	0.775	34.02	1.81×10^{-5}	0.835	1.46×10^4	/	88.97
		6	0.669	3.064×10^{-6}	0.90	47.96	3.06×10^{-6}	0.748	2.96×10^4	/	94.56
		12	0.785	9.752×10^{-7}	0.968	78.34	9.75×10^{-7}	0.730	4.01×10^4	/	95.99
	2	0.5	1.445	1.258×10^{-6}	1	86.81	1.26×10^{-6}	0.681	2.02×10^4	/	92.03
		2	1.103	1.861×10^{-6}	0.946	207.4	1.86×10^{-6}	0.698	3.99×10^4	/	95.96
		6	0.604	9.295×10^{-7}	1	70.81	9.30×10^{-7}	0.727	5.41×10^4	/	97.02
		12	0.409	7.136×10^{-7}	1	116	7.14×10^{-7}	0.766	7.71×10^4	/	97.91

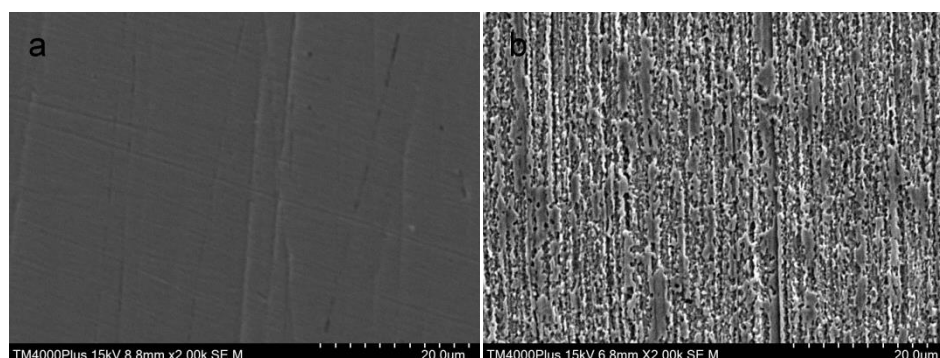
Table 2. Impedance parameters of bare copper and TMTA modified copper in 3.5wt% NaCl solution

C (mM)	Time(h)	$R_s(\Omega \text{ cm}^2)$	$Q_{film}(S\text{sncm}^{-2})$	n_1	$R_{film}(\Omega \text{ cm}^2)$	$Q_{dl}(S\text{sncm}^{-2})$	n_2	$R_{ct}(\Omega \text{ cm}^2)$	W	$\eta(\%)$
Bare		0.602	1.095×10^{-5}	1	105.8	1.21×10^{-4}	0.618	1.61×10^3	0.005968	/
TMTA-SAMS										
1	0.5	0.308	8.323×10^{-5}	0.6711	7357	1.311×10^{-3}	1	2.106×10^3	0.00065	23.33
	2	0.471	5.604×10^{-5}	0.7009	7279	1.425×10^{-5}	0.7491	1.02×10^4	0.00007	84.22
	6	0.759	1.884×10^{-6}	0.9709	110.9	2.726×10^{-5}	0.7441	1.27×10^4	0.00086	87.32
	12	0.702	1.02×10^{-6}	1	32.66	8.038×10^{-5}	0.565	1.59×10^4	0.00056	89.87
2	0.5	1.046	2.1×10^{-6}	1	37.39	1.236×10^{-4}	0.6412	6.39×10^3	0.00045	74.80
	2	1.208	1.662×10^{-6}	1	28.84	2.125×10^{-4}	0.5991	1.28×10^4	0.00061	87.42
	6	0.821	4.385×10^{-6}	0.8808	149.2	6.299×10^{-5}	0.6842	1.19×10^4	0.00055	79.77
	12	1.034	3.335×10^{-6}	0.8621	97.84	5.319×10^{-5}	0.6648	1.71×10^4	0.00058	90.05

3.4. Morphological examination

3.4.1. SEM analysis

Freshly polished copper, copper with TMTA SAMs, copper with MSDS SAMs, copper with MSDS SAMs soaked in 298k of 3.5wt% NaCl solution for 36 hours and SEM micrograph of freshly polished copper as shown in Figs.7. Show. All time involved in self-assembly is 7days. As shown in Fig.7a, the surface of the new polished copper is even and smooth with a small amount of sandpaper. The bare copper shown in Fig.7b is corroded by the etching solution, and the surface image becomes rough, this phenomenon is more obvious than in Fig.7a. It can be seen from Fig. 7c that there are many depressions on the surface of TMTA modified copper. Obviously this is the corrosion of the etching solution. The notch is sparse than bare copper, indicating that TMTA modified copper has certain corrosion inhibition performance in 3.5wt% NaCl solution. Apparently, Fig.7d shows the microscopic surface of the copper modified by MSDS. The surface is smooth with only a few tiny grooves. The washed and dried sodium chloride adheres to the copper surface and is not immersed in the copper as in the former. MSDS modified copper has excellent corrosion inhibition performance in 3.5wt% NaCl solution. This is consistent with the situation illustrated by electrochemical impedance spectroscopy.



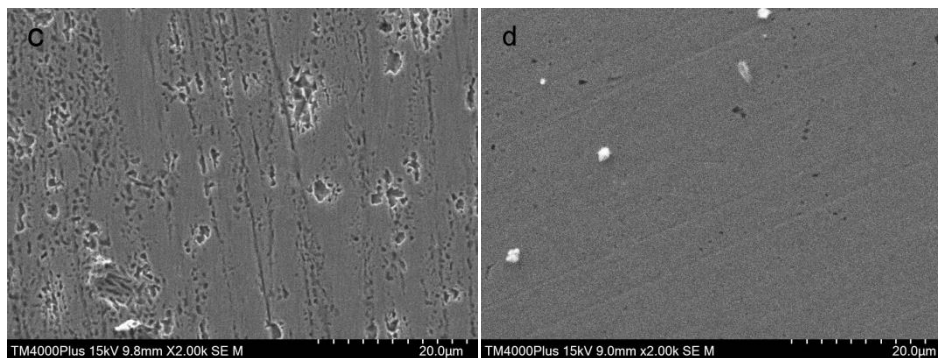


Figure 7. SEM graphs of copper surface: fresh bare copper (a);copper surface dipped in 3.5% NaCl solutions untreated with SAM(b), and treated with different SAMs. TMTA SAMs(c) and MSDS SAMs(d) for 7 days at 298 K.

3.4.2. AFM analysis

Figs. 8 are a further characterization of the microstructure of the copper surface by the AFM pattern of the copper surface, demonstrating the corrosion inhibition of copper by MSDS. Figs. 8a, 8b are AFM images of fresh polished copper and bare copper immersed in a 3.5 wt% NaCl solution for 2 days on a copper surface, respectively. These images are more stereoscopic and intuitive. Fig. 10a is a three-dimensional AFM pattern of the fresh polished copper surface, which has a flat surface with only a small amount of slight scratches. Conversely, the copper surface immersed in fresh sodium chloride solution for 48 hours became extremely rough, with many raised peaks and irregular depressions, apparently not due to the polished copper surface. This indicates that the copper surface has undergone severe corrosion. Figs. 8c, 8d are AFM model diagrams of copper modified by TMTA and MSDS after soaking in fresh sodium chloride solution for 48 hours, respectively. Figs. 8c, 8d show slight bulges in addition to the scratches that appear, which is micro-etching of the copper surface. Fig. 8c is more severe than Fig. 8d, indicating that the MSDS modified copper surface is more TMP-modified copper. The surface is more resistant to chloride ion attack, which is consistent with the electrochemical performance of the two materials assembled on the copper surface in the sodium chloride system, and is consistent with the results of scanning electron microscopy. [33-37]

The average height of the overall images of the copper surface are demonstrated in picture 9. The surface roughness (RMS) value is obtained from the height profile to more clearly reflect the corrosion of the copper surface. For fresh polished copper surfaces, the average value of RMS only achieves 4.23 nm. However, the RMS value of bare copper after soaking for 2 days in 3.5% sodium chloride solution is up to 67.32 nm. When the surface of the copper is modified, the roughness of the copper surface is significantly reduced, especially after the MSDS modified copper sample is immersed in a 3.5% sodium chloride solution for 2 days, the RMS drops to 23.13 nm, in the same case, after the RMS of the TMTA modified copper surface was also reduced to 52.65 nm. AFM test results agree well with electrochemical and SEM results.

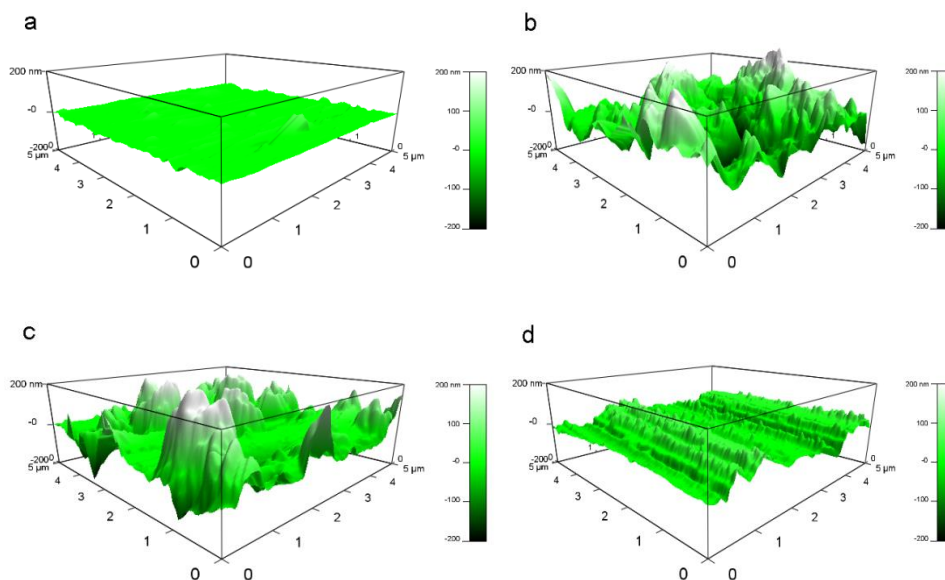


Figure 8. AFMgraphs of copper surface: fresh bare copper (a); copper surface dipped in 3.5% NaCl solutions untreated with SAM (b), and treated with different SAMs. TMTA SAMs (c) and MSDS SAMs (d) for 2 days at 298 K.

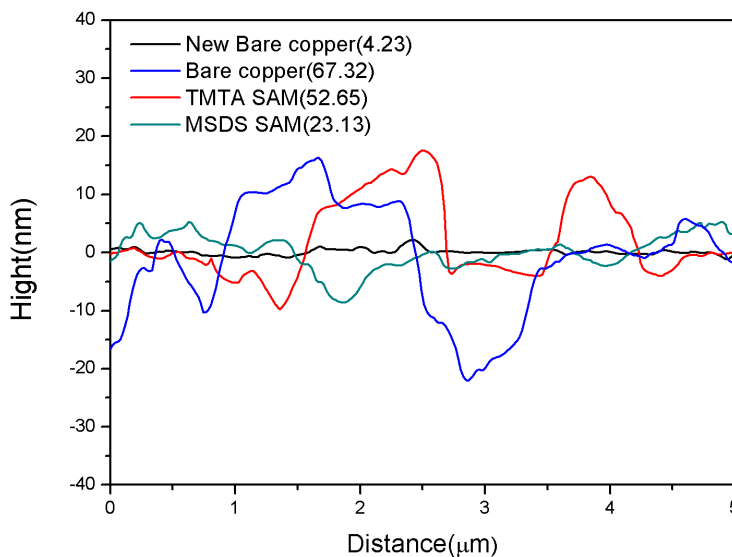


Figure 9. Random copper surface height profile: fresh bare copper; copper surface immersed in 3.5% NaCl solutions untreated with SAM, and treated with different SAMs. TMTA SAMs and MSDS SAMs for 48 h at 298 K.

3.5. Test of Contact angle

Comparison of the hydrophobicity of MSDS SAMs by contact angle measurement, Figs 10a and 10b are static water contact angle images of bare copper surface and MSDS SAMs covered copper surface, respectively. The image shows that the MSDS SAMs covered copper surface is more

hydrophobic than the bare copper surface, indicating that the MSDS self-assembly on the copper surface is successful. The results of the Infrared test were consistent. The volume of this drop is $5\mu\text{l}$, and the repeated measurement results are very reproducible. When the polar functional group is immobilized on the copper surface, the non-polar groups will turn to the solution, which will form a hydrophobic interface, resulting in a larger value of the contact angle.[38]

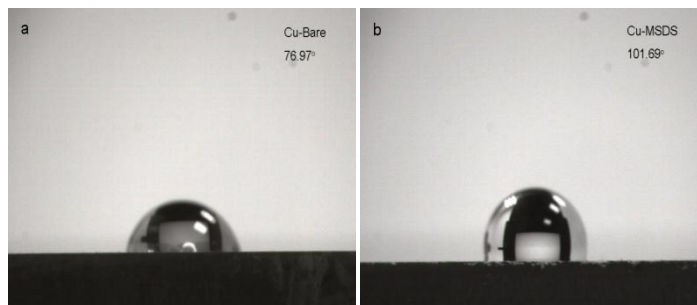


Figure 10. Multiple measurements of contact angle mean: bare copper (a); MSDS modified copper (b).

3.6. Theoretical calculation

3.6.1. Quantum chemical study

The relationship between the self-assembled membrane molecules and the corrosion inhibition mechanism of the membrane molecules is deeply revealed, by using the quantum chemical calculation method.[39] In the optimized molecular structure diagram, the density distributions of the highest occupied molecular orbital and the lowest unoccupied molecular orbital are shown in Figs.11a and 11b, respectively. Some vital parameters, LUMO energy and HOMO energy, energetic disparity, dipole distance, are calculated separately. Table 3 shows these important values. From the Angle of molecular E_{homo} has the ability to provide electronic E_{lumo} have the ability to accept electronic, this creates a high density distribution of electron cloud, from HOMO figure can be clearly seen in multivariate distribution around the N S on the ring with a large number of electrons, LUMO figure in N atomic distribution around a mass of electrons, resulting in the self-assembled film adsorption on the metal surface. In fact, the smaller $\Delta E (\Delta E = E_{\text{LUMO}} - E_{\text{HOMO}} = -0.19914\text{eV})$ will form a stronger adsorption on the metal surface. It has been reported in the literature that the larger μ is the stronger the adsorption of organic matter on the metal surface. [40] This is consistent with other characterization methods.

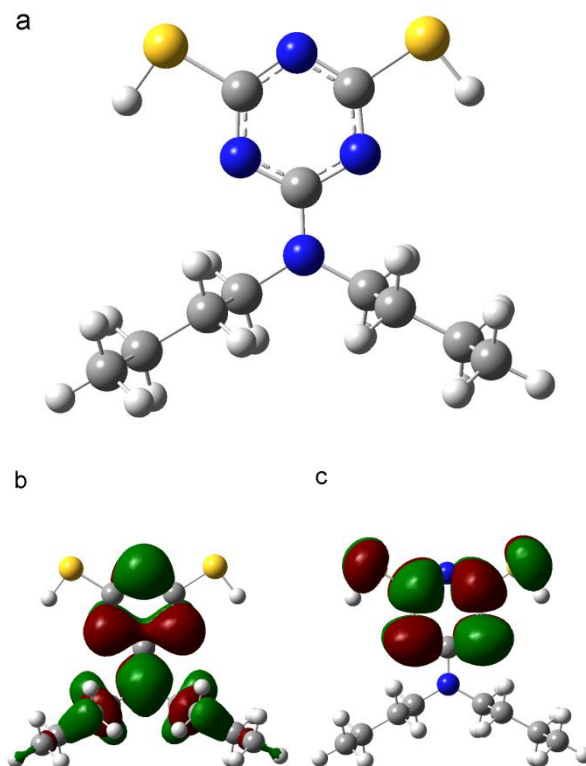


Figure 11. Optimized structure (a), HOMO (b), LUMO (c); density distribution of MSDS.

Table 3. Quantum chemical relevant parameters for the MSDS.

E_{HOMO} (eV)	E_{LUMO} (eV)	ΔE (eV)	μ (D)
-0.24407	-0.04493	0.19914	5.1049

3.6.2. Molecular dynamic simulation

Inhibitor research has expanded to atomic levels, for example, molecular kinematics simulations are used to generate molecular understanding of processes associated with corrosion inhibition mechanisms, this tool is widely trusted and accepted. The adsorption mechanism of MSDS on copper surface was researched by molecular dynamics (MD) simulation.[41] Figs.12a and 12b are side and top views, respectively, of an adsorption equilibrium configuration of MSDS molecules on a Cu(111) surface. It is obvious that all the inhibitors are almost parallel to the copper surface, whether in the side view or in the top view, and the parallel direction of the inhibitor can maximize the connection area between the inhibitor molecule and the copper, which maximizes Reduce corrosion on the copper surface. In addition, the relationship between the interaction energy between the copper (1,1,1) surface and the inhibitor molecule ($E_{\text{interaction}}$) is as follows

$$E_{\text{interact}} = E_{\text{tot}} - (E_{\text{subs}} + E_{\text{inh}}) \quad (8)$$

The total energy of the entire configuration is simply referred to as E_{tot} . The energy of water molecules and copper matrix is represented by E_{subs} . E_{inh} is the energy of MSDS. Calculated value of

interaction energy (E_{interact}) is -95.75 kJ / mol. The strong adsorption of MSDS to the copper surface is accompanied by a high negative energy interaction energy ($E_{\text{interaction}}$), which is consistent with the electrochemical test results.

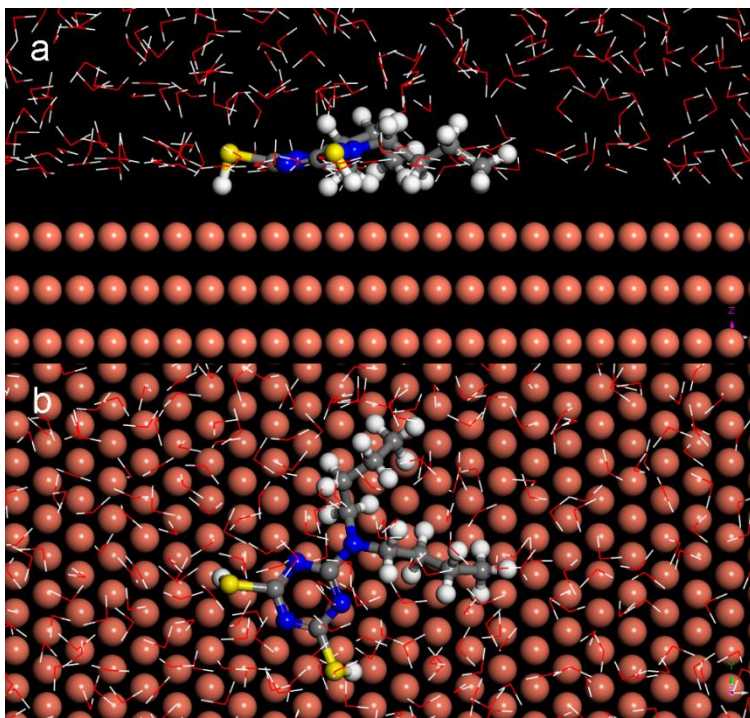


Figure 12. Side view (a) and top view (b); inhibitor molecules adsorbed on Cu(1,1,1) surface.

4. CONCLUSIONS

(1) Infrared spectroscopy (FT-IR) shows that MSDS self-assembled on copper surface.

(2) The polarization curve test showed that the corrosion of copper modified by MSDS in 3.5wt% NaCl solution was significantly weakened, mainly inhibiting the anode reaction.

(3) The EIS results manifest that the MSDS SAMs has a corrosion inhibition efficiency of 97.91% in 3.5% sodium chloride solution, an assembly time of 12 hours, and a MSDS concentration of 2 mM. Under the same conditions, the MSDS corrosion inhibition reaction is more violently than the analog TMTA.

(4) SEM and AFM images suggest that MSDSSAMs can inhibit copper corrosion well in 3.5% sodium chloride solution.

(5) Quantum chemical calculations and MD simulations show that the active adsorption sites of MSDS and copper surfaces are S, N and triazine rings.

(6) Self-assembled film can be explored to protect printed circuit board copper.

ACKNOWLEDGMENTS

This research was supported by National Natural Science Foundation of China (No. 21676035, 21878029) and sail plan of Guangdong, China (No. 2015YT02D025),

References

1. O. Geuli and D. Mandler, *Corros. Sci.*, 143(2018) 329-336.
2. S. Magdassi, M. Grouchko and A. Kamyshny, *Materials*, 3(2010) 4626-4638.
3. S. Yuan, S. O. Pehkonen, B. Liang, Y. P. Ting, K. G. Neoh and E. T. Kang, *Corros. Sci.*, 53(2011) 2738-2747.
4. Y. Zhang and Y. Chen, *Corrosion Engineering, Sci. Technol.*, 54(2018) 75-85.
5. E. Kowsari, S. Y. Arman, M. H. Shahini, H. Zandi, A. Ehsani, R. Naderi, *Corros. Sci.*, 112(2016) 73-85.
6. J. R. Xavier and R. Nallaiyan, *J. Solid State Electr.*, 16(2011) 391-402.
7. Y. Qiang, S. Fu, S. Zhang, S. Chen and X. Zou, *Corros. Sci.*, 140(2018) 111-121.
8. M. Behpour and N. Mohammadi, *Corros. Sci.*, 65(2012) 331-339.
9. Y. Qiang, S. Zhang, S. Xu and W. Li, *J. Colloid Interface Sci.*, 472(2016) 52-59.
10. J. Wang, Y. Qiang, L. Jiang, B. Xiang, S. Chen, S. Xing, Y. Wang and Y. Wang, *J. Mol. Liq.*, 271(2018) 959-969.
11. S. Chen, B. Xiang, S. Chen, X. Zou, Y. Zhou and J. Hou, *Appl. Surf. Sci.*, 456(2018) 25-36.
12. Y. Qiang, L. Guo, S. Zhang, W. Li, S. Yu and J. Tan, *Sci. Rep.*, 6(2016) 33305.
13. M. M. Motawea, *Int. J. Electrochem. Sci.*, 14 (2019) 1372-1387.
14. B. Tan, S. Zhang, Y. Qiang, L. Guo, L. Feng, C. Liao, Y. Xu and S. Chen, *J. Colloid Interface Sci.*, 526(2018) 268-280.
15. M. Scendo and M. Hepel, *Corros. Sci.*, 49(2007) 3381-3407.
16. I. H. Ali, *Int. J. Electrochem. Sci.*, 13(2018) 11580-11595.
17. T.-y. Weng, *Int. J. Electrochem. Sci.*, 13(2018) 11882-11894.
18. R. Zhang, *Int. J. Electrochem. Sci.*, 13(2018) 11526-11538.
19. Y. Qiang, S. Zhang, L. Guo, X. Zheng, B. Xiang and S. Chen, *Corros. Sci.*, 119(2017) 68-78.
20. B. Lin and Y. Zuo, *RSC Advances*, 9(2019) 7065-7077.
21. W. Chen, S. Hong, H. Q. Luo and N. B. Li, *J. Mater. Eng. Perform.*, 23(2013) 527-537.
22. Y. Qiang, S. Zhang, B. Tan and S. Chen, *Corros. Sci.*, 133(2018) 6-16.
23. N. Osaka, M. Ishitsuka and T. Hiaki, *J. Mol. Struct.*, 921(2009) 144-149.
24. L. Feng, S. Zhang, Y. Qiang, Y. Xu, L. Guo, L. Madkour and S. Chen, *Materials*, 11(2018)
25. Z. Khiati, A. A. Othman, M. Sanchez-Moreno, M. C. Bernard, S. Joiret, E. M. M. Sutter and V. Vivier, *Corros. Sci.*, 53(2011) 3092-3099.
26. S. Hong, W. Chen, H. Q. Luo and N. B. Li, *Corros. Sci.*, 57(2012) 270-278.
27. Y. Gong, Z. Wang, F. Gao, S. Zhang and H. Li, *Ind. Eng. Chem. Res.*, 54(2015) 12242-12253.
28. Y. Xu, S. Zhang, W. Li, L. Guo, S. Xu, L. Feng and L. H. Madkour, *Appl. Surf. Sci.*, 459(2018) 612-620.
29. M. Saadawy, *Arab. J. Sci. Eng.*, 41(2015) 177-190.
30. Y. Qiang, S. Zhang, S. Yan, X. Zou and S. Chen, *Corros. Sci.*, 126(2017) 295-304.
31. J. Zhang, L. Zhang and G. Tao, *J. Mol. Liq.*, 272(2018) 369-379.
32. F. Elmi, A. Gharakhani, S. Ghasemi and H. Alinezhad, *Prog. Org. Coat.*, 119(2018) 127-137.
33. M. Bagherzadeh and F. Jaberinia, *J. Alloy. Compd.*, 750(2018) 677-686.
34. J. Li, D. Chen, D. Zhang, Y. Wang, Y. Yu, L. Gao and M. Huang, *Colloid. Surface A.*, 550(2018) 145-154.
35. J. Bogan, A. Brady-Boyd, S. Armini, R. Lundy, V. Selvaraju and R. O'Connor, *Appl. Surf. Sci.*, 462(2018) 38-47.

36. S. Pareek, D. Jain, S. Hussain, A. Biswas, R. Shrivastava, S. K. Parida, H. K. Kisan, H. Lgaz, I.-M. Chung and D. Behera, *Chem. Eng. J.*, 258(2019)725-742.
37. B. Tan, S. Zhang, H. Liu, Y. Guo, Y. Qiang, W. Li, L. Guo, C. Xu and S. Chen, *J. Colloid Interf Sci.*, 538(2019)519-529.
38. S. Hu, Z. Chen and X. Guo, *Materials*, 11(2018)
39. P. Han, W. Li, H. Tian, X. Gao, R. Ding, C. Xiong and C. Chen, *J. Mol. Liq.*, 268(2018) 425-437.
40. W. Chen, S. Hong, H. B. Li, H. Q. Luo, M. Li and N. B. Li, *Corros. Sci.*, 61(2012)53-62.
41. B. Tan, S. Zhang, Y. Qiang, L. Feng, C. Liao, Y. Xu and S. Chen, *J. Mol. Liq.*, 248(2017) 902-910.

© 2019 The Authors. Published by ESG (www.electrochemsci.org). This article is an open access article distributed under the terms and conditions of the Creative Commons Attribution license (<http://creativecommons.org/licenses/by/4.0/>).